High-Performance Beampattern Synthesis via Linear Fractional Semidefinite Relaxation and Quasi-Convex Optimization

Xuejing Zhang, *Student Member, IEEE*, Zishu He, *Member, IEEE*, Xuepan Zhang, and Weilai Peng

***Abstract*— This paper presents a new method to synthesize high-performance beampatterns, with the aid of linear fractional semidefinite relaxation (LFSDR) technique and a quasi-convex optimization approach. We consider two beampattern synthesis problems. The first one is how to determine the weight vector to maximize the array gain (or equivalently, to minimize the gain loss in mainlobe), under the condition that the amplitude response satisfies specific requirements. The second one is how to minimize the notch level at a given region, on the premise of a permissible gain loss in mainlobe. To these ends, two nonconvex optimization problems are first formulated and then relaxed to their quasi-convex forms, by using the LFSDR technique. To further solve the resultant problems, the bisection method, which is commonly used in quasi-convex optimization, is adopted. Suboptimal solutions to the original nonconvex problems are finally obtained through eigenvalue decomposition or randomization manipulations. The proposed method performs well in both the cases described earlier. Moreover, our method is not limited to the array configurations and/or noise environments. Representative simulations are presented to demonstrate the effectiveness of the proposed method in high-performance beampattern synthesis.**

***Index Terms*— Beampattern synthesis, linear fractional semidefinite relaxation (LFSDR), mainlobe loss minimization, notch minimization, shape constraint, quasi-convex optimization.**

I. Introduction

ANTENNA arrays are widely used in many modern remote sensing, radar, and wireless communication systems [1]–[3]. Beampattern is one of the most important characteristics for assessing performance of an array. How to determine the complex weights for array elements to obtain a desired beampattern, i.e., beampattern synthesis [4]–[7], is a fundamental problem. As is known, the beampattern shape is important and has been widely considered in the literature. In practical applications, however, the array gain, which is proportional to the output signal-to-noise-ratio (SNR) as the input SNR fixed [8], directly affects the system performances, such as targets detecting/tracking, parameter estimation, and so on. Therefore, beampattern synthesis with both shape and array gain being considered is of great importance for practical antenna arrays.

Many beampattern synthesis approaches have been proposed during the past several decades. For instance, the classical Dolph–Chebychev synthesis technique obtains uniform sidelobes and a beamwidth that is the minimum possible for the given sidelobe level [9]. However, its application to arrays with arbitrary geometries or nonisotropic elements is not straightforward. Global optimization-based methods, such as genetic algorithm [10], simulated annealing method [11], and particle swarm optimization method [12], are applicable to nonuniformly spaced arrays. Nevertheless, the heavy computational load would limit their practical applications. Beampattern synthesis approaches developed on the basis of the adaptive array theory in [13] and [14] have no limitations on the array configurations. However, they are unable to control the beampattern precisely according to the required specifications. More importantly, some key parameters in these approaches are often selected in an *ad hoc* manner. Deterministic schemes on parameter selection need further investigation. Chou *et al.* [15] develop an efficient approach to synthesize the near-field pattern of an antenna array, by utilizing a global basis set to represent the excitation amplitude of the array with an additional phase impression to generate focused spot beam in the near zone. For a large planar array with periodic element spacing, low-sidelobe pattern is obtained in [16] by utilizing successive fast Fourier transform. And the quantization error is further considered in [17], in combination with the iterative Fourier transform method. A general design procedure is obtained in [18] to synthesize any type of pattern, such as sum, difference, and shaped beams, by using the Poisson sum expansion of the array factor. A fast pattern synthesis algorithm for conformal antenna arrays is presented in [19], which allows the simultaneous synthesis of the copolar and of the cross-polar array patterns, together with the control of the dynamic range ratio of the excitations.

As a powerful mathematical tool, the convex optimization theory has been successfully exploited to synthesize desirable beampatterns. For example, Lebret and Boyd [20] have shown how convex optimization can be utilized to design the optimal pattern for arbitrary antenna arrays. Semidefinite programming is employed in [21] to design nonuniform arrays with a desired magnitude response. Convex optimization is adopted in [22] to achieve a pattern that is arbitrarily upper

Manuscript received September 22, 2017; revised February 14, 2018; accepted April 25, 2018. Date of publication May 10, 2018; date of current version July 3, 2018. This work was supported by the National Nature Science Foundation of China under Grant 61671139 and Grant 61701499. *(Corresponding author: Xuepan Zhang.)*

X. Zhang, Z. He, and W. Peng are with the School of Communication and Information Engineering, University of Electronic Science and Technology of China, Chengdu 611731, China (e-mail: xjzhang7@163.com; zshe@uestc.edu.cn; lestinpwl@163.com).

X. Zhang is with the Qian Xuesen Laboratory of Space Technology, Beijing 100094, China (e-mail: zhangxuepan@qxslab.cn).

Color versions of one or more of the figures in this paper are available online at http://ieeexplore.ieee.org.

Digital Object Identifier 10.1109/TAP.2018.2835310

bounded while its polarization is optimized in a given angular region. Fuchs and Rondineau [23] present several procedures to synthesize array pattern while controlling the excitations, and find the ultimate solutions by using convex optimization technique. Note that although beampattern synthesis problems are usually nonconvex, convex optimization techniques are still of great use. By iteratively linearizing the nonconvex power pattern function, a series of convex subproblems is obtained in [24] and further solved using the second-order cone programming. By utilizing the symmetric geometries of linear and planar arrays, a conjugate symmetric weight vector is adopted in [25] such that the nonconvex lower bound constraints on the beampattern can be convexified. In [26], the semidefinite relaxation (SDR) technique [27] is employed to approximate the nonconvex constraints in the beampattern synthesis problem as convex. Consequently, a computationally efficient approach to the synthesis of shaped beams is devised. Apart from the aforementioned methods, there also exist some approaches attempting to synthesize patterns by using the embedded element pattern decomposition [28], utilizing the least-squares method [29]–[31], employing Hankel transformation and nonstochastic optimization [32], or with the aid of the array response control algorithms [33]–[37].

Notice that the above-mentioned approaches only focus on the shape of a beampattern, but ignore the consideration on array gain. In fact, array gain is directly related to the output SNR and power loss in mainlobe region, and has been deliberated for array designers. A beampattern being well designed in shape (i.e., sidelobe level, mainlobe width, and so on) may consume much power on individual element and result little radiation power in the desired direction. A few approaches have been presented to improve the array gain and reduce the energy loss in mainlobe. Dawoud and Anderson [38] attempted to improve the array gain by taking advantage of the polynomial optimization. However, this method is limited to uniformly spaced arrays and its extension to general configuration is still an open problem. In [39], the beam shaping approach minimizes the mainlobe loss under the constraint that the sidelobes are below a particular threshold, or minimizes the sidelobe level at a prescribed region under the given mainlobe loss constraint. This method designs a phase-only weight vector which does not ensure a high performance of the resulting beampattern.

In order to synthesize a high-performance beampattern with both shape and array gain considered, a new beampattern synthesis method is proposed in this paper, by using SDR and quasi-convex optimization. We address two commonly encountered beampattern synthesis problems as similarly considered in [39]. The first one concerns the determination of the weight vector, which minimizes the mainlobe loss under the constraint that the beampattern shape meets some specific requirements. The second problem can be regarded as the dual form of the first one, i.e., how to minimize the sidelobe level at given region(s) under the condition that the mainlobe shape and the array gain loss satisfy prescribed requirements. As shall be shown later, both these two problems are nonconvex and can be handled in similar manners. More specifically, the original formulation is first converted into a quasi-convex linear fractional SDR (LFSDR) problem [41]. On this basis, the bisection method [42]–[44] is adopted to obtain the optimal solution of the LFSDR problem. Finally, we extract a suboptimal solution of the original problem by using the eigenvalue decomposition (EVD) or Gaussian randomization. The proposed approach is not limited to a phase-only weight vector, and it performs well in both the two aforementioned cases. Moreover, the proposed method has no limitations on the noise structure and the array configuration.

This paper is organized as follows. In Section II, preliminaries are provided. The LFSDR and quasi-convex optimization are briefly introduced in Section III. Two beampattern synthesis problems are considered in Section IV. In Section V, numerical examples are conducted to demonstrate the performance of the proposed method, and conclusions are drawn in Section VI.

II. Preliminaries

Let us consider an N-element antenna array with arbitrary geometry. For convenience, we consider the 1-D array in this paper. However, the proposed method herein can be applied to the 2-D scenario. The steering vector associated with the direction θ is given as

$$\mathbf{a}(\theta) = [g_1(\theta)e^{j\phi_1(\theta)}, \cdots, g_N(\theta)e^{j\phi_N(\theta)}]^T \tag{1}$$

where $g_n(\theta)$ represents the radiation pattern of the nth element (we have $g_n(\theta) = 1$ when the antenna is isotropic), $\phi_n(\theta)$ stands for the phase delay of the nth element, $n = 1, \ldots, N$, $(\cdot)^T$ denotes the transpose operator, and $j = \sqrt{-1}$ is the imaginary unit. The normalized array power response is given as

$$B(\theta, \theta_0) = |\mathbf{w}^H\mathbf{a}(\theta)|^2/|\mathbf{w}^H\mathbf{a}(\theta_0)|^2 \tag{2}$$

where $\mathbf{w} = [w_1,\ w_2, \ldots, w_N]^T$ is the weight vector, $(\cdot)^H$ denotes conjugate transpose operator, and θ_0 stands for the direction of beam axis, which is also the incidence angle of the desired signal. The normalized array response $B(\theta, \theta_0)$ is important to an array system and has been well designed in quite a number of literatures.

In the case of one single signal, the array observation can be expressed as

$$\mathbf{x}(t) = \mathbf{x}_s(t) + \mathbf{x}_n(t) \tag{3}$$

where $\mathbf{x}_s(t)$ and $\mathbf{x}_n(t)$ stand for the signal component and the noise component, respectively. The covariance matrices of signal and noise can be, respectively, written as

$$\mathbf{R}_s = E\big[\mathbf{x}_s(t)\mathbf{x}_s^H(t)\big] = \sigma_s^2\mathbf{a}(\theta_0)\mathbf{a}^H(\theta_0) \tag{4}$$

$$\mathbf{R}_n = E\big[\mathbf{x}_n(t)\mathbf{x}_n^H(t)\big] = \sigma_n^2\Xi \tag{5}$$

where σ_s^2 and σ_n^2 are the powers of signal and noise, respectively. Ξ in (4) is positive semidefinite to characterize the structure of noise and is termed in [8] as the normalized noise covariance matrix. Clearly, the input SNR is given as

$$\mathrm{SNR_{in}} = \sigma_s^2/\sigma_n^2. \tag{6}$$

For a given weight vector $\mathbf{w}$, the array output can be written as $y(t) = \mathbf{w}^H \mathbf{x}(t)$, and the output power satisfies

$$E[|y(t)|^2] = \mathbf{w}^H \mathbf{R}_s \mathbf{w} + \mathbf{w}^H \mathbf{R}_n \mathbf{w} \tag{7}$$

where $\mathbf{w}^H \mathbf{R}_s \mathbf{w}$ and $\mathbf{w}^H \mathbf{R}_n \mathbf{w}$ represent the output components of signal and noise, respectively. Then, the output SNR can be expressed as

$$\mathrm{SNR}_{\mathrm{out}} = \frac{\mathbf{w}^H \mathbf{R}_s \mathbf{w}}{\mathbf{w}^H \mathbf{R}_n \mathbf{w}} = \frac{\sigma_s^2 \mathbf{w}^H \mathbf{a}(\theta_0)\mathbf{a}^H(\theta_0)\mathbf{w}}{\sigma_n^2 \mathbf{w}^H \Xi \mathbf{w}}. \tag{8}$$

It is known that one of the major tasks of an array is to improve the output SNR by adding signals coherently and noise incoherently [8]. The improvement is usually measured by the array gain, which is defined as the ratio of the output SNR and input SNR. According to (6) and (8), the array gain can be expressed as

$$G(\mathbf{w}) \triangleq \frac{\mathrm{SNR}_{\mathrm{out}}}{\mathrm{SNR}_{\mathrm{in}}} = \frac{\mathbf{w}^H \mathbf{a}(\theta_0)\mathbf{a}^H(\theta_0)\mathbf{w}}{\mathbf{w}^H \Xi \mathbf{w}}. \tag{9}$$

Clearly, maximizing $G(\mathbf{w})$ by finding an optimal weight vector (denoted by $\overline{\mathbf{w}}$ and termed as quiescent weight vector in the relevant literatures) is a so-called Rayleigh quotient problem [40], which can be solved by the generalized EVD of the matrix pencil $([\mathbf{a}(\theta_0)\mathbf{a}^H(\theta_0)], \Xi)$. More precisely, the weight vector $\overline{\mathbf{w}}$ that maximizes $G(\mathbf{w})$ satisfies

$$[\mathbf{a}(\theta_0)\mathbf{a}^H(\theta_0)]\overline{\mathbf{w}} = \lambda_1 \Xi \overline{\mathbf{w}} \tag{10}$$

where λ_1 is the maximum eigenvalue of the generalized EVD. It can be readily obtained from (10) that $\overline{\mathbf{w}}$ corresponds to the principal eigenvector of the matrix pencil $([\mathbf{a}(\theta_0)\mathbf{a}^H(\theta_0)], \Xi)$. Note that the following important inequality is satisfied for the quiescent weight vector $\overline{\mathbf{w}}$, that is,

$$G(\mathbf{w}) \le G(\overline{\mathbf{w}}) \quad \forall \mathbf{w} \in \mathbb{C}^N. \tag{11}$$

In addition, one can obtain $\overline{\mathbf{w}} = \mathbf{a}(\theta_0)$ in a Gaussian white noise environment, i.e., $\Xi = \mathbf{I}$.

In general, a weight vector $\mathbf{w}$ that is designed to make the normalized array response $B(\theta, \theta_0)$ satisfies the specific requirements will cause (more or less) gain loss. For this consideration, we attempt to investigate how to synthesize a desirable beampattern with both shape and array gain well performed. To this end, let us define a gain loss (or mainlobe loss) indicator to measure the array gain attenuation as

$$\mathrm{Loss}(\mathbf{w}) \triangleq G(\overline{\mathbf{w}})/G(\mathbf{w}). \tag{12}$$

Meanwhile, we can obtain the attenuated beampattern as

$$P(\theta, \theta_0) = B(\theta, \theta_0) \cdot \frac{G(\mathbf{w})}{G(\overline{\mathbf{w}})} = \frac{B(\theta, \theta_0)}{\mathrm{Loss}(\mathbf{w})} \tag{13}$$

which illustrates the gain loss intuitively as shall be shown in simulations later.

III. Linear Fractional Semidefinite Relaxation and Quasi-Convex Optimization

To be more self-contained, we introduce the LFSDR and quasi-convex optimization in this section.

A. Linear Fractional Semidefinite Relaxation

As shown in [41], LFSDR is a simple variant of SDR [27], which is a powerful and computationally efficient approximation technique for a host of difficult optimization problems.

1) SDR: Let us consider the following real-valued quadratically constrained quadratic program as

$$\min_{\mathbf{v} \in \mathbb{S}^n} \ \mathbf{v}^T \mathbf{C} \mathbf{v} \tag{14a}$$

$$\text{s.t.} \ \mathbf{v}^T \mathbf{B}_i \mathbf{v} \trianglerighteq_i d_i, \quad i = 1, \ldots, m \tag{14b}$$

where $\trianglerighteq_i$ can represent either $\ge, =,$ or $\le$ for each i, $\mathbf{C}, \mathbf{B}_i \in \mathbb{S}^n$, where $\mathbb{S}^n$ stands for the set of real symmetric $n \times n$ matrices, each d_i in (14) is real number for $\forall i = 1, \ldots, m$. An important observation is that

$$\mathbf{v}^T \mathbf{C} \mathbf{v} = \mathrm{tr}(\mathbf{C}\mathbf{v}\mathbf{v}^T), \quad \mathbf{v}^T \mathbf{B}_i \mathbf{v} = \mathrm{tr}(\mathbf{B}_i \mathbf{v}\mathbf{v}^T) \tag{15}$$

where $\mathrm{tr}(\cdot)$ denotes the trace of a matrix. On this basis, we introduce a new variable $\mathbf{V} = \mathbf{v}\mathbf{v}^T$ and reformulate the problem (14) as

$$\min_{\mathbf{V} \in \mathbb{S}^n} \ \mathrm{tr}(\mathbf{C}\mathbf{V}) \tag{16a}$$

$$\text{s.t.} \ \mathrm{tr}(\mathbf{B}_i \mathbf{V}) \trianglerighteq_i d_i, \ i = 1, \ldots, m \tag{16b}$$

$$\mathbf{V} \succeq \mathbf{0} \tag{16c}$$

$$\mathrm{rank}(\mathbf{V}) = 1. \tag{16d}$$

Note that the constraint $\mathrm{rank}(\mathbf{V}) = 1$ is imposed since $\mathrm{rank}(\mathbf{V}) = \mathrm{rank}(\mathbf{v}\mathbf{v}^T) = 1$. However, this constraint is nonconvex. The basic concept of SDR is dropping the rank constraint and relaxing the problem (16) as

$$\min_{\mathbf{V} \in \mathbb{S}^n} \ \mathrm{tr}(\mathbf{C}\mathbf{V}) \tag{17a}$$

$$\text{s.t.} \ \mathrm{tr}(\mathbf{B}_i \mathbf{V}) \trianglerighteq_i d_i, \quad i = 1, \ldots, m \tag{17b}$$

$$\mathbf{V} \succeq \mathbf{0}. \tag{17c}$$

This is a convex problem, and therefore, can be effectively solved by software packages [45].

Once the optimal solution to (17) (denoted by $\widehat{\mathbf{V}}$) has been obtained, a feasible solution to (14) can be extracted from $\hat{\mathbf{V}}$. Many approaches have been developed toward this purpose. For example, through EVD, we can get a potential solution of problem (14) as $\tilde{\mathbf{v}} = \sqrt{\sigma_1}\mathbf{u}_1$, where σ_1 is the largest eigenvalue of $\widehat{\mathbf{V}}$ and $\mathbf{u}_1$ is the corresponding eigenvector. One may also extract an approximate solution to (14) from $\widehat{\mathbf{V}}$ by using the so-called randomization approach [27].

2) LFSDR: As a modification of SDR, the LFSDR method [41] deals with the problems as follows:

$$\min_{\mathbf{v} \in \mathbb{R}^n} \ \frac{\mathbf{v}^T \mathbf{C} \mathbf{v}}{\mathbf{v}^T \mathbf{F} \mathbf{v}} \tag{18a}$$

$$\text{s.t.} \ \frac{\mathbf{v}^T \mathbf{B}_i \mathbf{v}}{\mathbf{v}^T \mathbf{D}_i \mathbf{v}} \trianglerighteq_i d_i, \quad i = 1, \ldots, m \tag{18b}$$

where $\mathbf{F}$ and $\mathbf{D}_i$ are semidefinite matrices for $i = 1, \ldots, m$. By defining $\mathbf{V} = \mathbf{v}\mathbf{v}^T$, one can rewrite (18) in terms of $\mathbf{V}$ as

$$\min_{\mathbf{V} \in \mathbb{S}^n} \ \frac{\mathrm{tr}(\mathbf{C}\mathbf{V})}{\mathrm{tr}(\mathbf{F}\mathbf{V})} \tag{19a}$$

$$\text{s.t.} \ \frac{\mathrm{tr}(\mathbf{B}_i \mathbf{V})}{\mathrm{tr}(\mathbf{D}_i \mathbf{V})} \trianglerighteq_i d_i, \quad i = 1, \ldots, m \tag{19b}$$

$$\mathbf{V} \succeq \mathbf{0} \tag{19c}$$
$$\text{rank}(\mathbf{V}) = 1. \tag{19d}$$

Similar to the SDR technique, problem (19) can be relaxed (by removing the rank-1 constraint) as

$$\min_{\mathbf{V}\in\mathbb{S}^n} \frac{\text{tr}(\mathbf{CV})}{\text{tr}(\mathbf{FV})} \tag{20a}$$
$$\text{s.t. } \text{tr}[(\mathbf{B}_i - d_i \cdot \mathbf{D}_i)\mathbf{V}] \trianglerighteq_i 0, \quad i = 1, \ldots, m \tag{20b}$$
$$\text{tr}(\mathbf{D}_i \mathbf{V}) \geq \beta, \quad i = 1, \ldots, m \tag{20c}$$
$$\mathbf{V} \succeq \mathbf{0} \tag{20d}$$

where $\beta > 0$ is a small number introduced to prevent the solution from being zero. Once the problem (20) has been solved, the EVD or randomization procedures can be applied to further obtain an approximation solution to the original problem (18). Unfortunately, the optimization problem (20) is nonconvex owing to the nonconvexity of $\text{tr}(\mathbf{CV})/\text{tr}(\mathbf{FV})$ in (20a), thus failing to be solved directly by convex toolbox [45]. Nevertheless, as it will be shown in Section II-B, the cost function (20a) is actually a quasi-convex function and the problem (20) can be solved via bisection method in polynomial time.

B. Quasi-Convex Function and Quasi-Convex Optimization

Quasi-convex function is an important kind of mapping, it is more generalized than the well-known convex function. Several quasi-convex optimization methods have been developed and utilized in the fields of signal processing [42] and machine learning [43]. In this section, preliminaries of the quasi-convex function and quasi-convex optimization problem are provided. The bisection algorithm [42]–[44], which is commonly adopted to deal with the quasi-convex optimization problems, is also introduced.

Definition 1: A function $f : \mathbb{R}^n \to \mathbb{R}$ is quasi-convex if its domain $\text{dom}(f)$ and all its α-sublevel sets defined as

$$S_\alpha = \{\mathbf{z} | \mathbf{z} \in \text{dom}(f), f(\mathbf{z}) \leq \alpha\} \tag{21}$$

are convex for $\forall \alpha \in \mathbb{R}$.

For illustration, the curve of a quasi-convex function is plotted in Fig. 1, where the dashed line segment $\overline{AB}$ that lies below the curve indicates the nonconvexity of the function. Obviously, a convex function has convex sublevel sets, and therefore, is quasi-convex, but the reverse may not hold true.

Definition 2: A function f is quasi-concave if $-f$ is quasi-convex. Moreover, if f is both quasi-convex and quasi-concave, we term it as quasi-linear.

From the above-mentioned definitions, it can be inferred that the cost function $f(\mathbf{V}) = \text{tr}(\mathbf{CV})/\text{tr}(\mathbf{FV})$ in (20) is quasi-linear.

As for the quasi-convex optimization problem, it has a form as

$$\min_{\mathbf{z}} f_0(\mathbf{z}) \tag{22a}$$
$$\text{s.t. } f_i(\mathbf{z}) \leq 0, \quad i = 1, \ldots, m \tag{22b}$$
$$h_i(\mathbf{z}) = 0, \quad i = 1, \ldots, p \tag{22c}$$

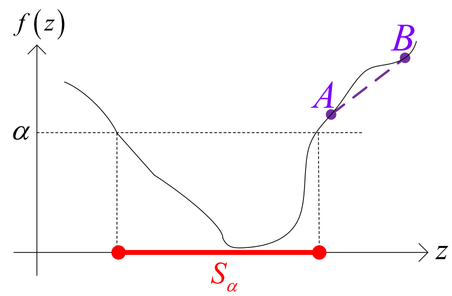

Fig. 1. Illustration of a quasi-convex function.

where $f_0(\mathbf{z})$ is quasi-convex, $f_i(\mathbf{z})$ is convex, and $h_i(\mathbf{z})$ is affine. To solve the problem (22), we reformulate it by using the epigraph representation [44] as

$$\min_{\mathbf{z}} \tau \tag{23a}$$
$$\text{s.t. } f_0(\mathbf{z}) \leq \tau \tag{23b}$$
$$f_i(\mathbf{z}) \leq 0, \quad i = 1, \ldots, m \tag{23c}$$
$$h_i(\mathbf{z}) = 0, \quad i = 1, \ldots, p. \tag{23d}$$

Note that the inequality constraints set $\{(\mathbf{z}, \tau) \big| f_0(\mathbf{z}) \leq \tau\}$ is not a convex set since f_0 is quasi-convex, and thus, the problem (23) is nonconvex. However, by fixing τ, the following problem of finding the feasible set is convex:

$$\text{find } \mathbf{z} \tag{24a}$$
$$\text{s.t. } f_0(\mathbf{z}) \leq \tau \tag{24b}$$
$$f_i(\mathbf{z}) \leq 0, \quad i = 1, \ldots, m \tag{24c}$$
$$h_i(\mathbf{z}) = 0, \quad i = 1, \ldots, p. \tag{24d}$$

It can be observed that the convex constraint set, denoted as $\mathcal{C}_\tau$, of the problem (24) can be expressed as

$$\mathcal{C}_\tau = \{\mathbf{z} \big| f_0(\mathbf{z}) \leq \tau, f_i(\mathbf{z}) \leq 0, i = 1, \ldots, m \quad h_i(\mathbf{z}) = 0, i = 1, \ldots, p\}. \tag{25}$$

Furthermore, it satisfies

$$\mathcal{C}_\tau \subseteq \mathcal{C}_s \quad \forall \tau \leq s. \tag{26}$$

More importantly, we have $\mathcal{C}_\tau \neq \emptyset$ for $\tau \geq \tau^*$ and $\mathcal{C}_\tau = \emptyset$ for $\tau < \tau^*$, where τ^* denotes the optimal value of the problem (23).

This observation (26) is significant to the idea for solving (22) or (23).

As aforementioned, the bisection method is a common technique to solve quasi-convex problem as (23). In brief, the optimization problem (23) is tackled via bisection method by iteratively decreasing τ until the problem (24) is feasible for $\tau \in [\tau^*, \tau^* + \epsilon]$, where ϵ is a preassigned small positive real number. More specifically, it is first assumed that τ^* lies within $[l, u]$, where both the lower bound l and the upper bound u of the interval are predetermined by the associated constraints. Next, we examine the feasibility of the midpoint $\tau = (l+u)/2$ according to the problem (24). If (24) is feasible, then we set $u = \tau$, otherwise, we update $l = \tau$. The convex feasibility problem (24) will be tested again by using the new interval

TABLE I
BISECTION METHOD FOR SOLVING QUASI-CONVEX PROBLEM (22)

Input	l, u, ϵ
Repeat	
	(1). Update $\tau = (l+u)/2$.
	(2). Solve the convex feasibility problem (24).
	(3). If the problem is feasible ($\mathcal{C} \neq \emptyset$), update $u = \tau$; otherwise update $l = \tau$.
Until	$u - l < \epsilon$
Output	$\mathbf{z}_{\text{opt}}$.

until $u - l \leq \epsilon$. The bisection method, for an ϵ-suboptimal solution, is summarized in Table I.

Now, recalling the optimization problem in (20), one finds that it is a special case of (22). Thus, it can be solved straightforwardly, by using the above-mentioned bisection method.

IV. HIGH-PERFORMANCE BEAMPATTERN SYNTHESIS VIA LFSDR AND QUASI-CONVEX OPTIMIZATION

In this section, we address two high-performance beampattern synthesis problems by using LFSDR, quasi-convex optimization and the bisection method.

A. Mainlobe Loss Minimization

In order to guarantee a high output SNR for an array system, it is desirable to minimize the mainlobe loss, or equivalently to maximize the array gain, under a specific shape constraint on beampattern. More specifically, the beampattern is often upper bounded by an envelop over some sidelobe regions, while in the mainlobe region, it usually requires both upper bound and also lower bound constraints on the beampattern. On the basis of these constraints on beampattern, we maximize the array gain by formulating the optimization problem as

$$\max_{\mathbf{w}} \; G(\mathbf{w}) \tag{27a}$$
$$\text{s.t. } B(\theta, \theta_0) \leq \rho(\theta), \quad \theta \in \mathbf{\Omega}_S \tag{27b}$$
$$l(\theta) \leq B(\theta, \theta_0) \leq u(\theta), \quad \theta \in \mathbf{\Omega}_M \tag{27c}$$

where $\rho(\theta)$ stands for the upper bound level at a specific sidelobe region $\mathbf{\Omega}_S$ and $l(\theta)$ and $u(\theta)$ represent the lower bound level and the upper bound level, respectively, of the mainlobe region $\mathbf{\Omega}_M$.

Then, according to the expressions of $B(\theta, \theta_0)$ in (2) and $G(\mathbf{w})$ in (9), the problem (27) can be rewritten as

$$\min_{\mathbf{w}} \; -\frac{\mathbf{w}^H \mathbf{a}(\theta_0)\mathbf{a}^H(\theta_0)\mathbf{w}}{\mathbf{w}^H \Xi \mathbf{w}} \tag{28a}$$
$$\text{s.t. } \frac{\mathbf{w}^H \mathbf{a}(\theta)\mathbf{a}^H(\theta)\mathbf{w}}{\mathbf{w}^H \mathbf{a}(\theta_0)\mathbf{a}^H(\theta_0)\mathbf{w}} \leq \rho(\theta), \quad \theta \in \mathbf{\Omega}_S \tag{28b}$$
$$l(\theta) \leq \frac{\mathbf{w}^H \mathbf{a}(\theta)\mathbf{a}^H(\theta)\mathbf{w}}{\mathbf{w}^H \mathbf{a}(\theta_0)\mathbf{a}^H(\theta_0)\mathbf{w}} \leq u(\theta), \quad \theta \in \mathbf{\Omega}_M. \tag{28c}$$

Note that the maximization problem (27) has been converted into a minimization problem. To proceed, let us define

$$\mathbf{A}_\theta \triangleq \mathbf{a}(\theta)\mathbf{a}^H(\theta) \in \mathbb{C}^{N\times N} \tag{29}$$

and then convert the problem (28) into the real domain for implementing consideration as

$$\min_{\widetilde{\mathbf{w}}} \; -\frac{\widetilde{\mathbf{w}}^H \widetilde{\mathbf{A}}_{\theta_0} \widetilde{\mathbf{w}}}{\widetilde{\mathbf{w}}^H \widetilde{\Xi} \widetilde{\mathbf{w}}} \tag{30a}$$
$$\text{s.t. } \frac{\widetilde{\mathbf{w}}^H \widetilde{\mathbf{A}}_{\theta} \widetilde{\mathbf{w}}}{\widetilde{\mathbf{w}}^H \widetilde{\mathbf{A}}_{\theta_0} \widetilde{\mathbf{w}}} \leq \rho(\theta), \quad \theta \in \mathbf{\Omega}_S \tag{30b}$$
$$l(\theta) \leq \frac{\widetilde{\mathbf{w}}^H \widetilde{\mathbf{A}}_{\theta} \widetilde{\mathbf{w}}}{\widetilde{\mathbf{w}}^H \widetilde{\mathbf{A}}_{\theta_0} \widetilde{\mathbf{w}}} \leq u(\theta), \quad \theta \in \mathbf{\Omega}_M \tag{30c}$$

where

$$\widetilde{\mathbf{A}}_\theta \triangleq \begin{bmatrix} \Re\{\mathbf{A}_\theta\} & -\Im\{\mathbf{A}_\theta\} \\ \Im\{\mathbf{A}_\theta\} & \Re\{\mathbf{A}_\theta\} \end{bmatrix} \in \mathbb{R}^{2N\times 2N} \tag{31a}$$
$$\widetilde{\Xi} \triangleq \begin{bmatrix} \Re\{\Xi\} & -\Im\{\Xi\} \\ \Im\{\Xi\} & \Re\{\Xi\} \end{bmatrix} \in \mathbb{R}^{2N\times 2N} \tag{31b}$$
$$\widetilde{\mathbf{w}} \triangleq \begin{bmatrix} \Re(\mathbf{w}^T) & \Im(\mathbf{w}^T) \end{bmatrix}^T \in \mathbb{R}^{2N} \tag{31c}$$

$\Re(\cdot)$ and $\Im(\cdot)$ return the real and imaginary parts of the bracketed term, respectively.

Applying the LFSDR technique to (30) yields the following relaxed problem:

$$\min_{\widetilde{\mathbf{W}}} \; -\frac{\text{tr}(\widetilde{\mathbf{A}}_{\theta_0}\widetilde{\mathbf{W}})}{\text{tr}(\widetilde{\Xi}\widetilde{\mathbf{W}})} \tag{32a}$$
$$\text{s.t. } \text{tr}[(\widetilde{\mathbf{A}}_\theta - \rho(\theta)\cdot\widetilde{\mathbf{A}}_{\theta_0})\widetilde{\mathbf{W}}] \leq 0, \quad \theta \in \mathbf{\Omega}_S \tag{32b}$$
$$\text{tr}[(\widetilde{\mathbf{A}}_\theta - u(\theta)\cdot\widetilde{\mathbf{A}}_{\theta_0})\widetilde{\mathbf{W}}] \leq 0, \quad \theta \in \mathbf{\Omega}_M \tag{32c}$$
$$\text{tr}[(\widetilde{\mathbf{A}}_\theta - l(\theta)\cdot\widetilde{\mathbf{A}}_{\theta_0})\widetilde{\mathbf{W}}] \geq 0, \quad \theta \in \mathbf{\Omega}_M \tag{32d}$$
$$\text{tr}(\widetilde{\mathbf{W}}) \geq \beta \tag{32e}$$
$$\widetilde{\mathbf{W}} \succeq \mathbf{0} \tag{32f}$$

where β can be assigned as a small positive value as discussed earlier in (20), $\widetilde{\mathbf{W}}$ is a rank-1 matrix defined as

$$\widetilde{\mathbf{W}} \triangleq \widetilde{\mathbf{w}}\widetilde{\mathbf{w}}^T \in \mathbb{R}^{2N\times 2N}. \tag{33}$$

Note that in (32), the nonconvex constraint $\text{rank}(\widetilde{\mathbf{W}}) = 1$ has been dropped for relaxation.

As described earlier in the last section, problem (32) is quasi-convex and can be expressed as

$$\min_{\widetilde{\mathbf{W}}} \; \tau \tag{34a}$$
$$\text{s.t. } \text{tr}[(\widetilde{\mathbf{A}}_{\theta_0} + \tau\cdot\widetilde{\Xi})\widetilde{\mathbf{W}}] \geq 0 \tag{34b}$$
$$\text{tr}[(\widetilde{\mathbf{A}}_\theta - \rho(\theta)\cdot\widetilde{\mathbf{A}}_{\theta_0})\widetilde{\mathbf{W}}] \leq 0, \quad \theta \in \mathbf{\Omega}_S \tag{34c}$$
$$\text{tr}[(\widetilde{\mathbf{A}}_\theta - u(\theta)\cdot\widetilde{\mathbf{A}}_{\theta_0})\widetilde{\mathbf{W}}] \leq 0, \quad \theta \in \mathbf{\Omega}_M \tag{34d}$$
$$\text{tr}[(\widetilde{\mathbf{A}}_\theta - l(\theta)\cdot\widetilde{\mathbf{A}}_{\theta_0})\widetilde{\mathbf{W}}] \geq 0, \quad \theta \in \mathbf{\Omega}_M \tag{34e}$$
$$\text{tr}(\widetilde{\mathbf{W}}) \geq \beta \tag{34f}$$
$$\widetilde{\mathbf{W}} \succeq 0. \tag{34g}$$

Accordingly, for a fixed τ, the following problem is convex:

$$\text{find } \widetilde{\mathbf{W}} \tag{35a}$$
$$\text{s.t. } \text{tr}[(\widetilde{\mathbf{A}}_{\theta_0} + \tau\cdot\widetilde{\Xi})\widetilde{\mathbf{W}}] \geq 0 \tag{35b}$$
$$\text{tr}[(\widetilde{\mathbf{A}}_\theta - \rho(\theta)\cdot\widetilde{\mathbf{A}}_{\theta_0})\widetilde{\mathbf{W}}] \leq 0, \quad \theta \in \mathbf{\Omega}_S \tag{35c}$$
$$\text{tr}[(\widetilde{\mathbf{A}}_\theta - u(\theta)\cdot\widetilde{\mathbf{A}}_{\theta_0})\widetilde{\mathbf{W}}] \leq 0, \quad \theta \in \mathbf{\Omega}_M \tag{35d}$$
$$\text{tr}[(\widetilde{\mathbf{A}}_\theta - l(\theta)\cdot\widetilde{\mathbf{A}}_{\theta_0})\widetilde{\mathbf{W}}] \geq 0, \quad \theta \in \mathbf{\Omega}_M \tag{35e}$$
$$\text{tr}(\widetilde{\mathbf{W}}) \geq \beta \tag{35f}$$

$$\widetilde{\mathbf{W}} \succeq 0. \tag{35g}$$

Moreover, recalling the inequality (11), we can find that $\tau \in [-G(\overline{\mathbf{w}}),\ 0]$, where the quiescent weight $\overline{\mathbf{w}}$ can be determined by (10). With this observation, the solution to (32), denoted as $\widetilde{\mathbf{W}}_1$, can thus be determined by using the bisection method as given in Table I. On this basis, the associated $\widetilde{\mathbf{w}}_1$ can be obtained via EVD or randomization as mentioned in Section III-A. Finally, from (31c), we can extract the weight vector as

$$\begin{aligned}\widehat{\mathbf{w}} &= [\widetilde{\mathbf{w}}_1(1), \ldots, \widetilde{\mathbf{w}}_1(N)]^T + j\,[\widetilde{\mathbf{w}}_1(N+1), \ldots, \widetilde{\mathbf{w}}_1(2N)]^T \\ &= \begin{bmatrix}\mathbf{I}_N & j\mathbf{I}_N\end{bmatrix}\widetilde{\mathbf{w}}_1 \end{aligned}\tag{36}$$

where $\widetilde{\mathbf{w}}_1(n)$ denotes the nth entry of $\widetilde{\mathbf{w}}_1$ and $\mathbf{I}_N$ denotes the $N \times N$ identity matrix.

B. Notch Minimization

Now, let us consider the notch minimization problem under the constraints of array gain and also the mainlobe shape. In this case, both the upper bound and the lower bound constraints are imposed on the responses of the mainlobe region. In addition, we constrain the array gain to be higher than a specific threshold. On this basis, we minimize the response level of a specific sidelobe sector where fixed interferences may exist. Mathematically, this problem can be formulated as

$$\min_{\mathbf{w}} \max_{\theta\in\Omega_S} B(\theta,\theta_0) \tag{37a}$$
$$\text{s.t. } l(\theta) \le B(\theta,\theta_0) \le u(\theta), \quad \theta \in \Omega_M \tag{37b}$$
$$G(\mathbf{w}) \ge \eta \tag{37c}$$

where Ω_S is the notch region where the response level needs to be minimized, Ω_M denotes the mainlobe region, $l(\theta)$ and $u(\theta)$ specify, respectively, the lower bound level and the upper bound level at Ω_M, and η is a user-defined permissible array gain.

The above-mentioned problem can be equivalently rewritten as

$$\min_{\mathbf{w}} \ \tau \tag{38a}$$
$$\text{s.t. } B(\theta,\theta_0) \le \tau,\ \theta \in \Omega_S \tag{38b}$$
$$l(\theta) \le B(\theta,\theta_0) \le u(\theta),\ \theta \in \Omega_M \tag{38c}$$
$$G(\mathbf{w}) \ge \eta. \tag{38d}$$

For the ease of implementing, we convert the problem (38) into the real domain as

$$\min_{\mathbf{w}} \ \tau \tag{39a}$$
$$\text{s.t. } \frac{\widetilde{\mathbf{w}}^H\widetilde{\mathbf{A}}_\theta\widetilde{\mathbf{w}}}{\widetilde{\mathbf{w}}^H\widetilde{\mathbf{A}}_{\theta_0}\widetilde{\mathbf{w}}} \le \tau, \quad \theta \in \Omega_S \tag{39b}$$
$$l(\theta) \le \frac{\widetilde{\mathbf{w}}^H\widetilde{\mathbf{A}}_\theta\widetilde{\mathbf{w}}}{\widetilde{\mathbf{w}}^H\widetilde{\mathbf{A}}_{\theta_0}\widetilde{\mathbf{w}}} \le u(\theta), \quad \theta \in \Omega_M \tag{39c}$$
$$\frac{\widetilde{\mathbf{w}}^H\widetilde{\mathbf{A}}_{\theta_0}\widetilde{\mathbf{w}}}{\widetilde{\mathbf{w}}^H\widetilde{\Xi}\widetilde{\mathbf{w}}} \ge \eta \tag{39d}$$

where $\widetilde{\mathbf{A}}_\theta$, $\widetilde{\Xi}$, and $\widetilde{\mathbf{w}}$ have been defined in (31). Then, by using the LFSDR approach, we can obtain a quasi-convex optimization problem as

$$\min_{\widetilde{\mathbf{W}}} \ \tau \tag{40a}$$
$$\text{s.t. } \mathrm{tr}[(\widetilde{\mathbf{A}}_\theta - \tau \cdot \widetilde{\mathbf{A}}_{\theta_0})\widetilde{\mathbf{W}}] \le 0, \quad \theta \in \Omega_S \tag{40b}$$
$$\mathrm{tr}[(\widetilde{\mathbf{A}}_\theta - u(\theta) \cdot \widetilde{\mathbf{A}}_{\theta_0})\widetilde{\mathbf{W}}] \le 0, \quad \theta \in \Omega_M \tag{40c}$$
$$\mathrm{tr}[(\widetilde{\mathbf{A}}_\theta - l(\theta) \cdot \widetilde{\mathbf{A}}_{\theta_0})\widetilde{\mathbf{W}}] \ge 0, \quad \theta \in \Omega_M \tag{40d}$$
$$\mathrm{tr}[(\eta \cdot \widetilde{\Xi} - \widetilde{\mathbf{A}}_{\theta_0})\widetilde{\mathbf{W}}] \le 0 \tag{40e}$$
$$\mathrm{tr}(\widetilde{\mathbf{W}}) \ge \beta \tag{40f}$$
$$\widetilde{\mathbf{W}} \succeq 0 \tag{40g}$$

where the rank-1 matrix $\widetilde{\mathbf{W}}$ has been defined in (33). As we have shown earlier, for a given τ in problem (40), the following convex optimization problem can be obtained:

$$\text{find } \widetilde{\mathbf{W}} \tag{41a}$$
$$\text{s.t. } \mathrm{tr}[(\widetilde{\mathbf{A}}_\theta - \tau \cdot \widetilde{\mathbf{A}}_{\theta_0})\widetilde{\mathbf{W}}] \le 0, \quad \theta \in \Omega_S \tag{41b}$$
$$\mathrm{tr}[(\widetilde{\mathbf{A}}_\theta - u(\theta) \cdot \widetilde{\mathbf{A}}_{\theta_0})\widetilde{\mathbf{W}}] \le 0, \quad \theta \in \Omega_M \tag{41c}$$
$$\mathrm{tr}[(\widetilde{\mathbf{A}}_\theta - l(\theta) \cdot \widetilde{\mathbf{A}}_{\theta_0})\widetilde{\mathbf{W}}] \ge 0, \quad \theta \in \Omega_M \tag{41d}$$
$$\mathrm{tr}[(\eta \cdot \widetilde{\Xi} - \widetilde{\mathbf{A}}_{\theta_0})\widetilde{\mathbf{W}}] \le 0 \tag{41e}$$
$$\mathrm{tr}(\widetilde{\mathbf{W}}) \ge \beta \tag{41f}$$
$$\widetilde{\mathbf{W}} \succeq 0. \tag{41g}$$

Moreover, a simple calculation results that $\tau \in [0, \gamma]$, where $\gamma = \max_{\theta\in\Omega_S} \overline{B}(\theta,\theta_0)$ with $\overline{B}(\theta,\theta_0)$ denoting the normalized response pattern of $\overline{\mathbf{w}}$. In the same manner, the bisection method can be utilized to get the optimal solution $\widetilde{\mathbf{W}}_2$ of the problem (41). Consequently, the obtained weight vector is given as

$$\widehat{\mathbf{w}} = \begin{bmatrix}\mathbf{I}_N & j\mathbf{I}_N\end{bmatrix}\mathbf{w}_2 \tag{42}$$

where $\mathbf{w}_2$ can be similarly obtained from $\widetilde{\mathbf{W}}_2$ via EVD or randomization procedure.

Remark: If we assume that the noise be white and Gaussian (i.e., $\Xi = \mathbf{I}$), and impose a phase-only constraint on the weight vector, then one can find that $\mathbf{w}^H\Xi\mathbf{w}$ is a constant with known value. Thus, the resulting problem can be solved by using the SDR technique [27]. This is exactly what literature [39] had discussed. In addition, a minimax cost function [i.e., (37a)] is adopted in the notch minimization case to result a uniform notch level, which is not well guaranteed in [39]. Above all, the proposed approach can be regarded as a generalization of the phase-only method in [39]. The phase-only constraint is unnecessary for the devised method and a uniform notch level can be obtained in the notch minimization case.

V. Numerical Results

In this section, representative simulations are carried out to validate the proposed method under the aforementioned two scenarios. For convenience, the Gaussian white noise is assumed, then we know that the quiescent weight $\overline{\mathbf{w}}$ equal to $\mathbf{a}(\theta_0)$. To illustrate the mainlobe losses of the synthesized beampatterns, we consider the attenuated beampattern $P(\theta,\theta_0)$ as defined in (13). In addition, we set $\beta = 0.1$ and $\epsilon = 10^{-6}$ for all the simulations. The variable `cvx_status` in CVX toolbox [45] is used to check the status of convex feasibility problem when implementing the bisection method, and the EVD manipulation is selected to extract a solution afterward. For comparison purpose, the phase only method in [39], convex programming (CP) in [20], the A^2RC method

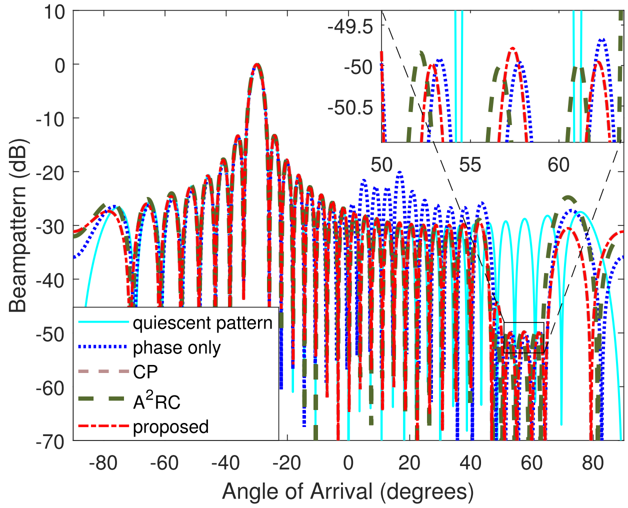

Fig. 2. Beampattern comparison for mainlobe loss minimization by using an ULA.

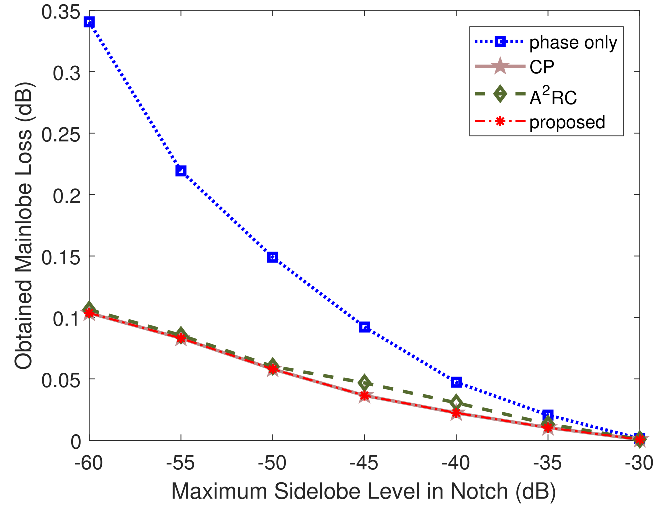

Fig. 3. Curves of mainlobe loss versus the maximum sidelobe level in notch.

in [47], and the concave–convex procedure (CCP) method in [49]–[51] are also tested if available.

A. Mainlobe Loss Minimization

In this section, we first specify the requirements on the beampattern shape, and then minimize the mainlobe loss to obtain a high array gain. Two different configurations are considered as shown in the following.

1) Uniform Linear Array With Uniform Sidelobe at One Single Region: In the first example, a linearly half-wavelength-spaced array with 32 isotropic elements is considered. The beampattern is assumed to steer to $\theta_0 = -30^\circ$. The desired sidelobe level is expected to be lower than -50 dB at the angle sector $\mathbf{\Omega}_S = [50^\circ,\ 65^\circ]$ and no other requirements elsewhere.

Fig. 2 shows the synthesized beampatterns in this case. From Fig. 2, it can be clearly seen that all the methods tested achieve desirable sidelobe levels at the given sector $\mathbf{\Omega}_S$. Moreover, one can find that the proposed method obtains the same beampattern as the CP method. When comparing the array gain, the resulting mainlobe loss of the proposed method is 0.058 dB, which is less than the corresponding values of the phase-only method and the A^{2}RC method. The effectiveness of the proposed method is thus well validated.

As pointed out in [39], there are necessarily tradeoffs between the depth of notches and the gain losses in mainlobe. Fig. 3 displays the obtained mainlobe losses when varying the notch levels from -60 to -30 dB, with other parameters unchanged. From Fig. 3, we learn that the higher level in notch region, the less mainlobe loss can be obtained. This result is suitable for all the methods tested. The resulting mainlobe losses of the proposed method are less than those of the other methods, for the given sidelobe levels in notch. Moreover, we can see that the mainlobe losses approximate to be zeros as the notch levels being close to -30 dB, which is the corresponding level of the quiescent pattern in the angle sector $\mathbf{\Omega}_S$, as shown in Fig. 2. In this case, the resulting weight vectors of different methods degrade to the quiescent weight $\overline{\mathbf{w}}$, which has no array gain loss.

TABLE II
ELEMENT LOCATIONS OF THE NONUNIFORM LINEAR ARRAY AND THE RESULTING WEIGHTS OF THE PROPOSED METHOD

n	$x_n(\lambda)$	w_n	n	$x_n(\lambda)$	w_n
1	0.00	$0.1038e^{+j1.6074}$	11	5.15	$0.7634e^{-j2.3479}$
2	0.45	$0.2107e^{+j2.0508}$	12	5.68	$0.8781e^{-j1.6678}$
3	0.92	$0.2704e^{+j2.4490}$	13	6.23	$0.9308e^{-j1.1390}$
4	1.35	$0.2777e^{-j3.1135}$	14	6.68	$0.9216e^{-j0.6140}$
5	1.98	$0.1933e^{-j2.8021}$	15	7.25	$1.0000e^{+j0.0000}$
6	2.41	$0.0949e^{-j1.9877}$	16	7.80	$0.7046e^{+j0.5811}$
7	3.02	$0.0275e^{+j1.8551}$	17	8.25	$0.7108e^{+j1.1360}$
8	3.62	$0.3082e^{+j2.2844}$	18	8.88	$0.5279e^{+j1.7313}$
9	4.12	$0.3849e^{+j2.8386}$	19	9.26	$0.2592e^{+j2.3173}$
10	4.52	$0.5748e^{-j2.8941}$	20	9.80	$0.1914e^{+j2.5509}$

2) Random Linear Array With Nonuniform Sidelobes and a Flat-Top Mainlobe: To further examine the performance of the proposed method in mainlobe loss minimization, we consider a 20-element nonuniform spaced linear array. The array element locations are provided in Table II. We set the beam axis as $\theta_0 = 10^\circ$. The desired sidelobe level is nonuniform, i.e., it varies with the angle θ. Specifically, the notch region is $\mathbf{\Omega}_S = [-40^\circ,\ -20^\circ] \cup [50^\circ,\ 60^\circ]$, the sidelobe level is expected to be lower than -30 dB if $\theta \in [-40^\circ,\ -20^\circ]$ and lower than -40 dB for θ in the interval $[50^\circ, 60^\circ]$. In addition, a flat-top mainlobe is required and the ripple is expected to be less than 0.5 dB at the mainlobe region $[5^\circ,\ 15^\circ]$.

Since the CP method does not work in this case, we thus compare our method with the phase only method [39], the A^{2}RC method [47], and the CCP method [49]–[51]. The resulting beampatterns are depicted in Fig. 4 and the obtained weightings of the proposed method are listed in Table II. From Fig. 4, it can be seen that both the phase-only method and the A^{2}RC method cannot form flat-top mainlobes, although the resulting sidelobe levels may have satisfied the preassigned requirements. The proposed method and the CCP method have obtained desirable shapes in the prescribed regions. When comparing the mainlobe loss, the resulting loss of the proposed method is 8.1034 dB, which is less than the

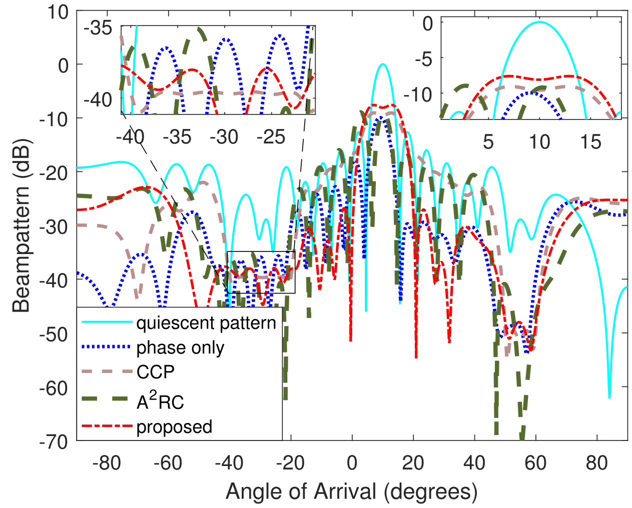

Fig. 4. Simulation result for a random linear array with nonuniform sidelobes and a flat-top mainlobe.

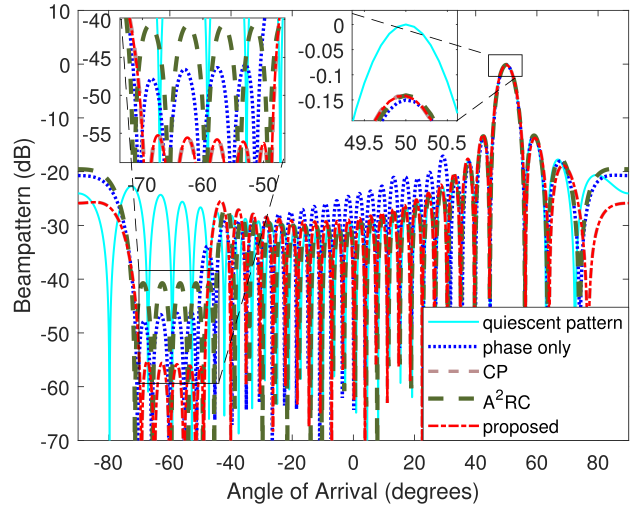

Fig. 5. Notch minimization using an ULA with 32 isotropic elements.

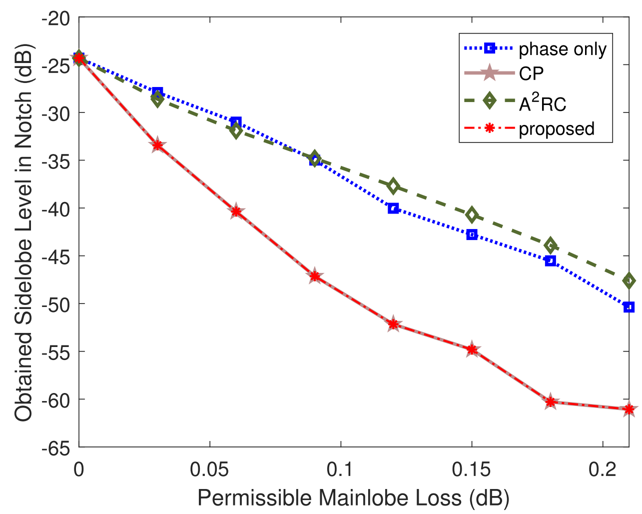

Fig. 6. Curves of the obtained notch level versus the permissible loss in mainlobe.

9.5637 dB of the CCP method. The performance degradation of the CCP method may be caused by its raised sidelobe responses, see for example, the responses at the angle sectors $[-20°, 0°] \cup [20°, 40°]$.

B. Notch Minimization

In this section, we present simulations to validate the performance of the proposed method in notch minimization.

1) Uniform Linear Array: In this example, an uniform linear array (ULA) with 32 isotropic elements is considered. The beam axis is set at $\theta_0 = 50°$. The permissible mainlobe loss is taken as $\eta = 0.15$ dB, and the notch region is $\Omega_S = [-70°, -50°]$ where the array response levels are expected to be minimized. In this case, we do not impose specific constraints on the responses of the mainlobe region.

Fig. 5 plots the simulation results of various methods. It can be observed that the resulting losses in mainlobe are all satisfied as desired. As for the notch levels, a uniform level with -55 dB is obtained by using either the proposed method or the CP method, while the obtained maximum notch levels are -41 and -40 dB, respectively, for the phase only method and the A^{2}RC method. Since the proposed method obtains the deepest notch with a qualified mainlobe loss, one can see that it outperforms the other methods.

The similar to the simulation in Section V-A, we also investigate the performance improvement of the proposed method, by varying the permissible mainlobe loss from 0 to 0.21 dB, and then plotting the curves of the resulting notch levels in Fig. 6, with other parameters unaltered. From Fig. 6, it can be clearly seen that a larger permitted gain loss corresponds to a deeper sidelobe notch, for all approaches. For the given permissible mainlobe losses, the resulting notch levels of the proposed method and the CP method are less than those of the phase-only method and the A^{2}RC method. Moreover, when η is set as 0 dB, i.e., no gain loss is permitted, all the resulting notch levels are -25 dB, which is exactly the maximum response level of the quiescent pattern in the region Ω_S. In this case, all the methods tested degenerate into the quiescent weighting method.

2) Nonisotropic Linear Random Array: In this scenario, we consider a 33-element nonisotropic linear random array, which was also described in [46]–[48]. The individual pattern for the nth element is given as

$$g_n(\theta) = \frac{\cos[\pi l_n \sin(\theta + \zeta_n)] - \cos(\pi l_n)}{\cos(\theta + \zeta_n)} \tag{43}$$

where ζ_n and l_n represent the orientation and length of the element. More description of the array can be found in Table III, where the sensor position x_n is also specified. We steer the beam to $\theta_0 = 30°$ and take the permissible mainlobe loss as $\eta = 3$ dB. The notch region is taken as $\Omega_S = [-40°, -20°]$. In addition, a flat-top mainlobe is expected in the angle sector $\Omega_M = [27°, 33°]$, and the ripple is restricted to be less than 0.5 dB.

Fig. 7 displays the synthesized beampatterns and Table III lists the resulting weightings of the proposed method. Clearly,

TABLE III

PARAMETERS OF THE NONISOTROPIC RANDOM ARRAY AND THE OBTAINED WEIGHTINGS BY THE PROPOSED METHOD

n	$x_n(\lambda)$	$l_n(\lambda)$	ζ_n(deg)	w_n
1	0.00	0.25	0.0	$0.1056e^{+j2.2608}$
2	0.50	0.25	0.5	$0.2617e^{-j2.4626}$
3	1.00	0.24	5.0	$0.1727e^{-j1.0891}$
4	1.55	0.20	-32	$0.1863e^{+j0.7930}$
5	2.09	0.26	-3.2	$0.2430e^{+j2.6422}$
6	2.69	0.27	10	$0.1893e^{-j2.1606}$
7	3.14	0.23	1.0	$0.1390e^{-j0.1584}$
8	3.60	0.24	0.0	$0.1391e^{+j0.8851}$
9	4.10	0.25	0.0	$0.0501e^{+j3.0359}$
10	4.60	0.21	7.0	$0.0234e^{-j1.3225}$
11	5.11	0.28	6.0	$0.0633e^{+j2.6352}$
12	5.58	0.30	4.4	$0.2378e^{-j2.4550}$
13	6.06	0.29	0.0	$0.1922e^{-j0.9758}$
14	6.67	0.19	1.0	$0.2288e^{+j1.0383}$
15	7.24	0.22	-2.1	$0.2571e^{+j3.0083}$
16	7.89	0.22	3.0	$0.3897e^{-j1.4684}$
17	8.31	0.25	0.0	$0.5155e^{+j0.0435}$
18	8.81	0.25	0.0	$0.6165e^{+j1.5552}$
19	9.31	0.24	5.0	$0.6068e^{+j3.1385}$
20	9.76	0.26	4.7	$0.6728e^{-j1.7307}$
21	10.31	0.27	-8.9	$1.0000e^{+j0.0000}$
22	10.85	0.28	3.0	$0.8706e^{+j1.7303}$
23	11.38	0.25	3.2	$0.7953e^{-j2.9267}$
24	11.94	0.25	2.8	$0.7807e^{-j1.1240}$
25	12.48	0.25	2.9	$0.7228e^{+j0.5502}$
26	13.04	0.23	1.5	$0.6808e^{+j2.2951}$
27	13.54	0.27	0.7	$0.7820e^{-j2.3567}$
28	14.04	0.28	0.3	$0.8424e^{-j0.8633}$
29	14.54	0.24	0.0	$0.6225e^{+j0.8365}$
30	15.11	0.24	0.4	$0.3799e^{+j2.4982}$
31	15.62	0.25	-20	$0.6609e^{-j2.0837}$
32	16.14	0.26	0.8	$0.3616e^{-j0.4376}$
33	16.63	0.25	-9.6	$0.1342e^{+j1.0571}$

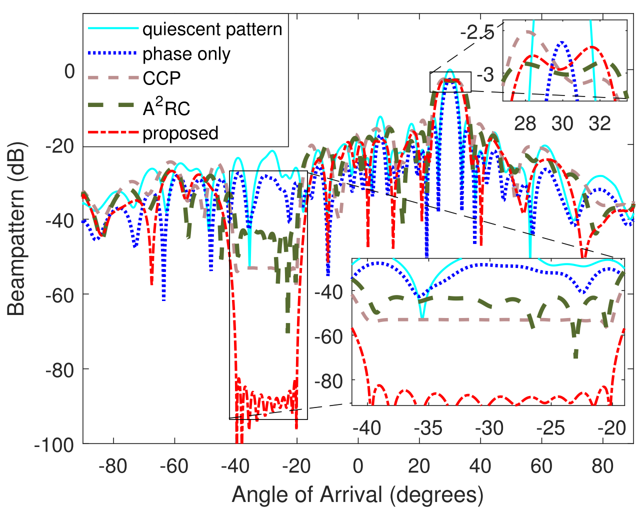

Fig. 7. Notch minimization using a nonisotropic linear random array.

the phase only method does not shape a desirable flat-top beampattern in the mainlobe region and its resulting notch level at Ω_S is rather high, although the obtained gain loss in mainlobe is qualified. The CCP method, A^2RC method, and the proposed method have synthesized satisfactory beampatterns in the preassigned mainlobe region, and their resulting gain losses also meet the requirements. When comparing the obtained notch levels, the CCP method results a uniform notch below -54 dB. In the sidelobe region Ω_S, the resulting maximal level of the A^2RC method is about -44 dB. As for the proposed method, the notch level is lower than -80 dB, which is greatly less than those of both the CCP method and the A^2RC method. Thus, the promising performance of the proposed method is clearly verified when it acts on a linear random array with nonisotropic elements.

VI. CONCLUSION

In this paper, the LFSDR and quasi-convex optimization have been applied to the synthesis of high-performance array beampatterns. Two important beampattern synthesis problems, i.e., mainlobe loss minimization and notch minimization, have been considered. Specifically, the LFSDR approach is first applied to relax and further convert the original problems to their corresponding quasi-convex formulations. Then, the bisection method, which is a mature technology for solving quasi-convex optimization problem, is utilized to find out the corresponding solutions of the quasi-convex formulations. Finally, we obtain the ultimate weight vectors via EVD or randomization manipulation. The proposed method works well for arbitrary arrays and has no limitation on the structure of noise covariance matrix. Representative examples have been carried out to illustrate the superiority of the proposed approach. As a future work, we shall consider the extension of LFSDR and quasi-convex optimization approaches to synthesize high-performance array beampatterns under uncertainties, and study how to reduce the possible high computation complexities of related operations in the devised method.

REFERENCES

[1] O. M. Bucci, L. Crocco, R. Scapaticci, and G. Bellizzi, "On the design of phased arrays for medical applications," *Proc. IEEE*, vol. 104, no. 3, pp. 633–648, Mar. 2016.

[2] J. E. Stailey and K. D. Hondl, "Multifunction phased array radar for aircraft and weather surveillance," *Proc. IEEE*, vol. 104, no. 3, pp. 649–659, Mar. 2016.

[3] J. Corcoles and M. A. Gonzalez, "Efficient combined array thinning and weighting for pattern synthesis with a nested optimization scheme," *IEEE Trans. Antennas Propag.*, vol. 60, no. 11, pp. 5107–5117, Nov. 2012.

[4] D. P. Scholnik, "A parameterized pattern-error objective for large-scale phase-only array pattern design," *IEEE Trans. Antennas Propag.*, vol. 64, no. 1, pp. 89–98, Jan. 2016.

[5] L. Di Palma, A. Clemente, L. Dussopt, R. Sauleau, P. Potier, and P. Pouliguen, "Radiation pattern synthesis for monopulse radar applications with a reconfigurable transmitarray antenna," *IEEE Trans. Antennas Propag.*, vol. 64, no. 9, pp. 4148–4154, Sep. 2016.

[6] J. Córcoles, "Reactively loaded array pattern synthesis as a quadratically constrained quadratic program," *IEEE Trans. Antennas Propag.*, vol. 63, no. 11, pp. 5219–5224, Nov. 2015.

[7] M. S. Hossain, G. N. Milford, M. C. Reed, and L. C. Godara, "Robust efficient broadband antenna array pattern synthesis techniques," *IEEE Trans. Antennas Propag.*, vol. 62, no. 9, pp. 4537–4546, Sep. 2014.

[8] H. K. Van Trees, *Optimum Array Processing*. New York, NY, USA: Wiley, 2002.

[9] C. L. Dolph, "A current distribution for broadside arrays which optimizes the relationship between beam width and side-lobe level," *Proc. IRE*, vol. 34, no. 6, pp. 335–348, Jun. 1946.

[10] K. Chen, X. Yun, Z. He, and C. Han, "Synthesis of sparse planar arrays using modified real genetic algorithm," *IEEE Trans. Antennas Propag.*, vol. 55, no. 4, pp. 1067–1073, Apr. 2007.

[11] V. Murino, A. Trucco, and C. S. Regazzoni, "Synthesis of unequally spaced arrays by simulated annealing," *IEEE Trans. Signal Process.*, vol. 44, no. 1, pp. 119–122, Jan. 1996.

[12] D. W. Boeringer and D. H. Werner, "Particle swarm optimization versus genetic algorithms for phased array synthesis," *IEEE Trans. Antennas Propag.*, vol. 52, no. 3, pp. 771–779, Mar. 2004.

[13] C. A. Olen and R. T. Compton, Jr., "A numerical pattern synthesis algorithm for arrays," *IEEE Trans. Antennas Propag.*, vol. 38, no. 10, pp. 1666–1676, Oct. 1990.

[14] P. Y. Zhou and M. A. Ingram, "Pattern synthesis for arbitrary arrays using an adaptive array method," *IEEE Trans. Antennas Propag.*, vol. 47, no. 5, pp. 862–869, May 1999.

[15] H.-T. Chou, N.-N. Wang, H.-H. Chou, and J.-H. Qiu, "An effective synthesis of planar array antennas for producing near-field contoured patterns," *IEEE Trans. Antennas Propag.*, vol. 59, no. 9, pp. 3224–3233, Sep. 2011.

[16] W. P. M. N. Keizer, "Fast low-sidelobe synthesis for large planar array antennas utilizing successive fast Fourier transforms of the array factor," *IEEE Trans. Antennas Propag.*, vol. 55, no. 3, pp. 715–722, Mar. 2007.

[17] W. P. M. N. Keizer, "Low sidelobe phased array pattern synthesis with compensation for errors due to quantized tapering," *IEEE Trans. Antennas Propag.*, vol. 59, no. 12, pp. 4520–4524, Dec. 2011.

[18] H. Oraizi and M. Fallahpour, "Sum, difference and shaped beam pattern synthesis by non-uniform spacing and phase control," *IEEE Trans. Antennas Propag.*, vol. 59, no. 12, pp. 4505–4511, Dec. 2011.

[19] M. Comisso and R. Vescovo, "Fast co-polar and cross-polar 3D pattern synthesis with dynamic range ratio reduction for conformal antenna arrays," *IEEE Trans. Antennas Propag.*, vol. 61, no. 2, pp. 614–626, Feb. 2013.

[20] H. Lebret and S. Boyd, "Antenna array pattern synthesis via convex optimization," *IEEE Trans. Signal Process.*, vol. 45, no. 3, pp. 526–532, Mar. 1997.

[21] F. Wang, V. Balakrishnan, P. Y. Zhou, J. J. Chen, R. Yang, and C. Frank, "Optimal array pattern synthesis using semidefinite programming," *IEEE Trans. Signal Process.*, vol. 51, no. 5, pp. 1172–1183, May 2003.

[22] B. Fuchsand and J. J. Fuchs, "Optimal polarization synthesis of arbitrary arrays with focused power pattern," *IEEE Trans. Antennas Propag.*, vol. 59, no. 12, pp. 4512–4519, Dec. 2011.

[23] B. Fuchs and S. Rondineau, "Array pattern synthesis with excitation control via norm minimization," *IEEE Trans. Antennas Propag.*, vol. 64, no. 10, pp. 4228–4234, Oct. 2016.

[24] K. M. Tsui and S. C. Chan, "Pattern synthesis of narrowband conformal arrays using iterative second-order cone programming," *IEEE Trans. Antennas Propag.*, vol. 58, no. 6, pp. 1959–1970, Jun. 2010.

[25] S. E. Nai, W. Ser, Z. L. Yu, and H. Chen, "Beampattern synthesis for linear and planar arrays with antenna selection by convex optimization," *IEEE Trans. Antennas Propag.*, vol. 58, no. 12, pp. 3923–3930, Dec. 2010.

[26] B. Fuchs, "Application of convex relaxation to array synthesis problems," *IEEE Trans. Antennas Propag.*, vol. 62, no. 2, pp. 634–640, Feb. 2014.

[27] Z.-Q. Luo, W.-K. Ma, A. M.-C. So, Y. Ye, and S. Zhang, "Semidefinite relaxation of quadratic optimization problems," *IEEE Signal Process. Mag.*, vol. 27, no. 3, pp. 20–34, May 2010.

[28] K. Yang, Z. Zhao, Z. Nie, J. Ouyang, and Q. H. Liu, "Synthesis of conformal phased arrays with embedded element pattern decomposition," *IEEE Trans. Antennas Propag.*, vol. 59, no. 8, pp. 2882–2888, Aug. 2011.

[29] I. D. Dotlic and A. J. Zejak, "Arbitrary antenna array pattern synthesis using minimax algorithm," *Electron. Lett.*, vol. 37, no. 4, pp. 206–208, Feb. 2001.

[30] F. Wang, R. Yang, and C. Frank, "A new algorithm for array pattern synthesis using the recursive least squares method," *IEEE Signal Process. Lett.*, vol. 10, no. 8, pp. 235–238, Aug. 2003.

[31] Z. Shi and Z. Feng, "A new array pattern synthesis algorithm using the two-step least-squares method," *IEEE Signal Process. Lett.*, vol. 12, no. 3, pp. 250–253, Mar. 2005.

[32] R. Eirey-Perez, J. A. Rodriguez-Gonzalez, and F. J. Ares-Pena, "Synthesis of array radiation pattern footprints using radial stretching, Fourier analysis, and Hankel transformation," *IEEE Trans. Antennas Propag.*, vol. 60, no. 4, pp. 2106–2109, Apr. 2012.

[33] X. Zhang, Z. He, B. Liao, X. Zhang, and W. Peng, "Pattern synthesis for arbitrary arrays via weight vector orthogonal decomposition," *IEEE Trans. Signal Process.*, vol. 66, no. 5, pp. 1286–1299, Mar. 2018.

[34] X. Zhang, Z. He, B. Liao, X. Zhang, and W. Peng, "Pattern synthesis with multipoint accurate array response control," *IEEE Trans. Antennas Propag.*, vol. 65, no. 8, pp. 4075–4088, Aug. 2017.

[35] X. Zhang, Z. He, X. Zhang, X. Chen, and W. Peng, "Pattern synthesis for arbitrary arrays by accurately controlling response level," in *Proc. IEEE Radar Conf. (RadarConf)*, May 2017, pp. 0106–0111.

[36] X. Zhang, Z. He, X.-G. Xia, B. Liao, X. Zhang, and Y. Yang. (Dec. 2017). "OPARC: Optimal and precise array response control algorithm—Part I: Fundamentals." [Online]. Available: https://arxiv.org/abs/1712.10088

[37] X. Zhang, Z. He, X.-G. Xia, B. Liao, X. Zhang, and Y. Yang. (Dec. 2017). "OPARC: Optimal and precise array response control algorithm—Part II: Multi-points and applications." [Online]. Available: https://arxiv.org/abs/1712.10090

[38] M. M. Dawoud and A. P. Anderson, "Design of superdirective arrays with high radiation efficiency," *IEEE Trans. Antennas Propag.*, vol. AP-26, no. 6, pp. 819–823, Nov. 1978.

[39] P. J. Kajenski, "Phase only antenna pattern notching via a semidefinite programming relaxation," *IEEE Trans. Antennas Propag.*, vol. 60, no. 5, pp. 2562–2565, May 2012.

[40] G. Strang, *Linear Algebra and Its Applications*, 4th ed. New York, NY, USA: Wellesley Cambridge Press, 2005.

[41] T. H. Chang, C. W. Hsin, W. K. Ma, and C. Y. Chi, "A linear fractional semidefinite relaxation approach to maximum-likelihood detection of higher-order QAM OSTBC in unknown channels," *IEEE Trans. Signal Process.*, vol. 58, no. 4, pp. 2315–2326, Apr. 2010.

[42] V. Havary-Nassab, S. Shahbazpanahi, A. Grami, and Z.-Q. Luo, "Distributed beamforming for relay networks based on second-order statistics of the channel state information," *IEEE Trans. Signal Process.*, vol. 56, no. 9, pp. 4306–4316, Sep. 2008.

[43] Q. Ke and T. Kanade, "Quasiconvex optimization for robust geometric reconstruction," *IEEE Trans. Pattern Anal. Mach. Intell.*, vol. 29, no. 10, pp. 1834–1847, Oct. 2007.

[44] S. Boyd and L. Vandenberghe, *Convex Optimization*. Cambridge, U.K.: Cambridge Univ. Press, 2004.

[45] *CVX: MATLAB Software for Disciplined Convex Programming*, CVX Res., Inc, San Ramon, CA, USA, Sep. 2012.

[46] C.-C. Tseng and L. J. Griffiths, "A simple algorithm to achieve desired patterns for arbitrary arrays," *IEEE Trans. Signal Process.*, vol. 40, no. 11, pp. 2737–2746, Nov. 1992.

[47] X. Zhang, Z. He, B. Liao, X. Zhang, Z. Cheng, and Y. Lu, "A^2RC: An accurate array response control algorithm for pattern synthesis," *IEEE Trans. Signal Process.*, vol. 65, no. 7, pp. 1810–1824, Apr. 2017.

[48] B. Fuchs and J. J. Fuchs, "Optimal narrow beam low sidelobe synthesis for arbitrary arrays," *IEEE Trans. Antennas Propag.*, vol. 58, no. 6, pp. 2130–2135, Jun. 2010.

[49] A. L. Yuille and A. Rangarajan, "The concave-convex procedure," *Neural Comput.*, vol. 15, no. 4, pp. 915–936, 2003.

[50] T. Lipp and S. Boyd, "Variations and extension of the convex–concave procedure," *Optim. Eng.*, vol. 17, pp. 263–287, Jun. 2016.

[51] O. Mehanna, K. Huang, B. Gopalakrishnan, A. Konar, and N. D. Sidiropoulos, "Feasible point pursuit and successive approximation of non-convex QCQPs," *IEEE Signal Process. Lett.*, vol. 22, no. 7, pp. 804–808, Jul. 2015.

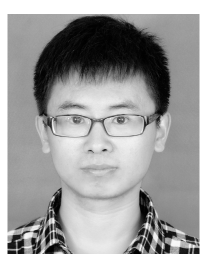

Xuejing Zhang (S'17) was born in Hebei, China. He received the B.S. degree in electrical engineering from Huaqiao University, Xiamen, China, and the M.S. degree in signal and information processing from Xidian University, Xi'an, China, in 2011 and 2014, respectively. He is currently pursuing the Ph.D. degree in signal and information processing with the Department of Electronic Engineering, University of Electronic Science and Technology of China, Chengdu, China.

From 2014 to 2015, he was a Research Engineer with Allwinner Inc., Zhuhai, China, where he was involved in algorithmic research. Since 2017, he has been a Visiting Student with the University of Delaware, Newark, DE, USA. His current research interests include array signal processing, optimization theory, and machine learning.

Zishu He (M'11) was born in Chengdu, China, in 1962. He received the B.S., M.S., and Ph.D. degrees in signal and information processing from the University of Electronic Science and Technology of China (UESTC), Chengdu, in 1984, 1988, and 2000, respectively.

He is currently a Professor of signal and information processing with the School of Electronic Engineering, UESTC. His current research interests include array signal processing, digital beam forming, the theory on multiple-input multiple-output (MIMO) communication and MIMO radar, adaptive signal processing, and interference cancellation.

Xuepan Zhang was born in Hebei, China. He received the B.S. and Ph.D. degrees in electrical engineering from the National Laboratory of Radar Signal Processing, Xidian University, Xi'an, China, in 2010 and 2015, respectively.

He is currently a Principal Investigator with the Qian Xuesen Laboratory of Space Technology, Beijing, China. His current research interests include synthetic aperture radar, ground moving target indication, and deep learning.

Weilai Peng received the B.Eng. degree in electronic engineering from the University of Electronic Science and Technology of China, Chengdu, China, in 2015, where he is currently pursuing the Ph.D. degree in electronic engineering.

His current research interests include array signal processing and multiple-input multiple-outpu radar.